

Ion Coulomb crystals as Analog quantum simulators

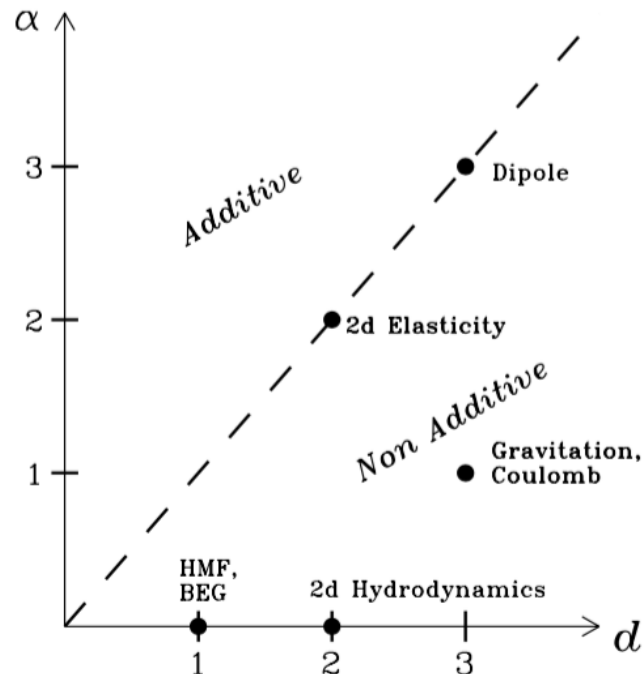
Giovanna Morigi
Universität des Saarlandes
Theoretische Physik

Long-range interactions

Potential scales with $1/r^a$
with exponent $a < \text{dimension } d$

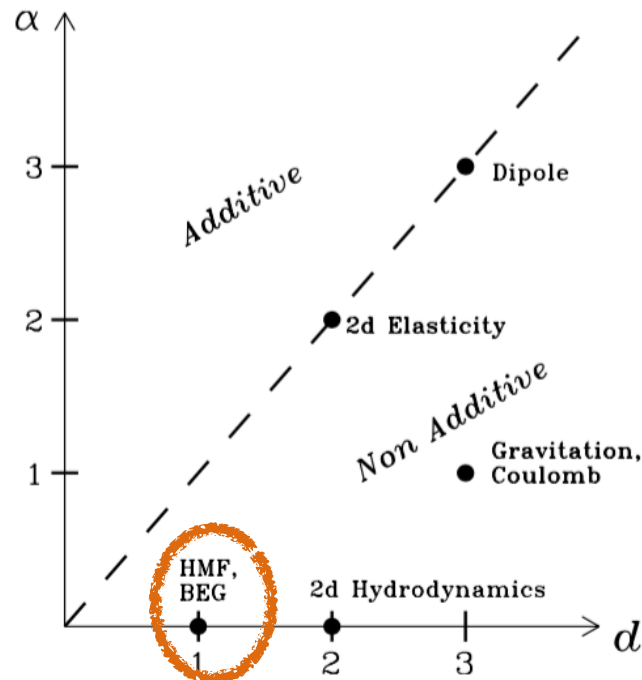
Long-range interactions

Potential scales with $1/r^a$
with exponent $a < \text{dimension } d$



Long-range interactions

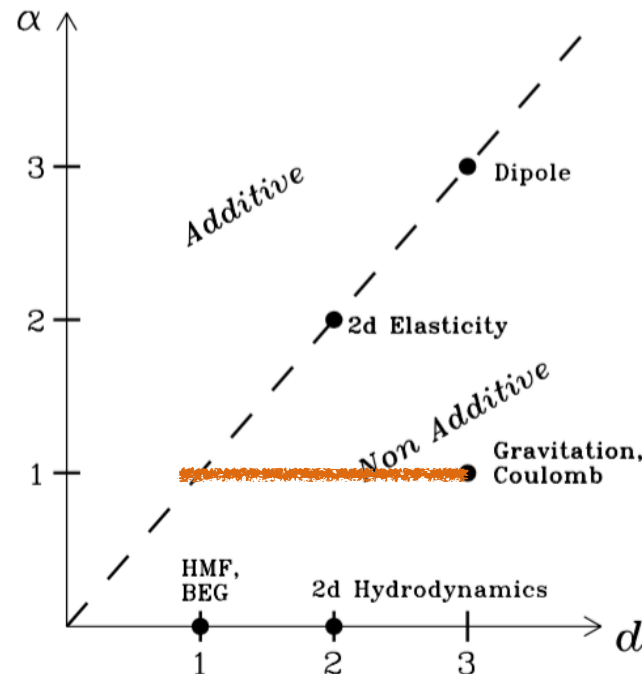
Potential scales with $1/r^a$
with exponent $a < \text{dimension } d$



Cavity Quantum Electrodynamics
Trapped ions (effective models)

Long-range interactions

Potential scales with $1/r^a$
with exponent $a < \text{dimension } d$



one-component plasmas

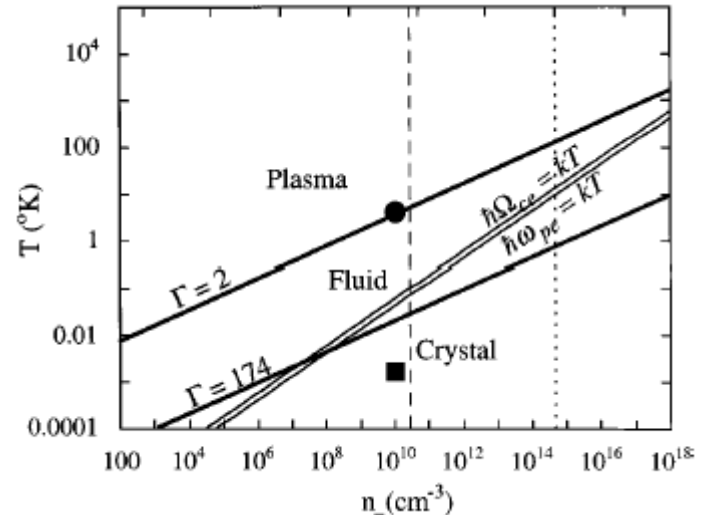
One-component plasma (homogeneous system, 3D)

Coupling parameter: $\Gamma = e^2 / akT$

$a = (3/4\pi n)^{1/3}$ Wigner-Seitz radius

Strong correlations: $\Gamma \gg 1$

Crystallization (transition to spatial order): $\Gamma = 174$



Coulomb systems in a lab

Bragg Diffraction from Crystallized Ion Plasmas

W. M. Itano,* J. J. Bollinger, J. N. Tan,† B. Jelenković,‡
X.-P. Huang, D. J. Wineland

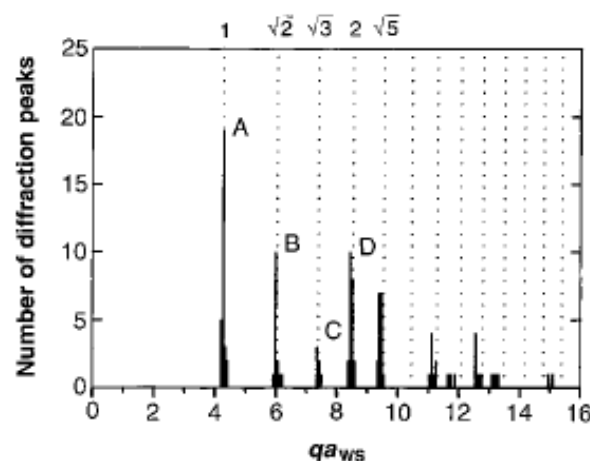
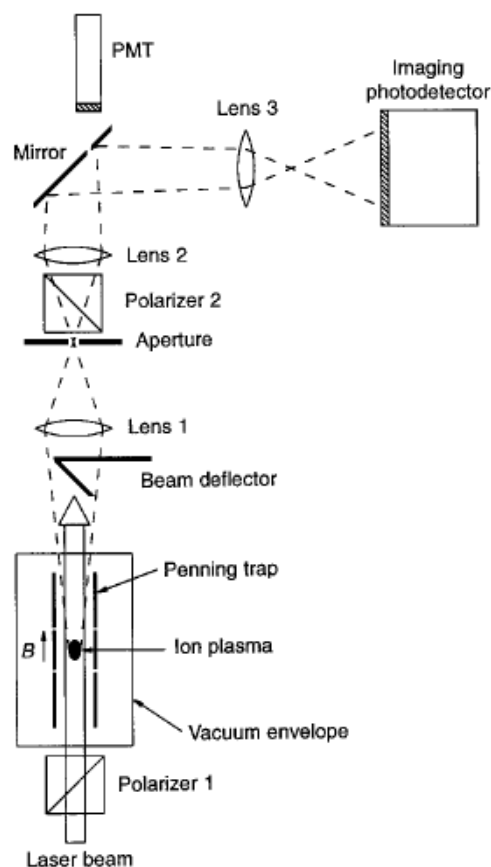


Fig. 3. Histogram representing the numbers of peaks (not intensities) observed as a function of qa_{ws} , where $\mathbf{q} = \mathbf{k}_s - \mathbf{k}_i$ is the difference between the incident (\mathbf{k}_i) and scattered (\mathbf{k}_s) photon wave vectors. We analyzed 30 Bragg diffraction patterns from two approximately spherical plasmas having 270,000 and 470,000 ions. The dotted lines show the expected peak positions, normalized to the center of gravity of the peak at A ($\{110\}$ Bragg reflections).

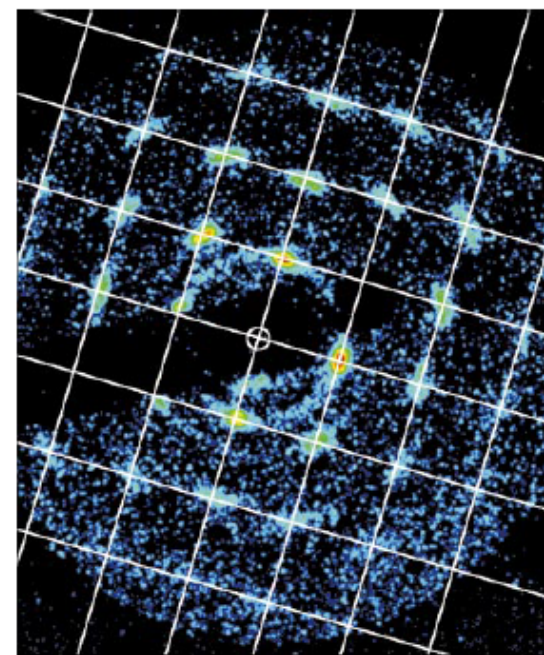


Fig. 4. Time-resolved Bragg diffraction pattern of the same plasma as in Fig. 2. Here and in Figs. 5 and 6 the small open circle marks the position of the undeflected laser beam. A bcc lattice, aligned along a $\langle 100 \rangle$ axis, would generate a spot at each intersection of the grid lines overlaid on the image. The grid spacing corresponds to an angular deviation of 2.54×10^{-2} rad. Here, $\omega_r = 2\pi \times 125.6$ kHz, $n_0 = 3.83 \times 10^{19}$ cm $^{-3}$, $N = 5 \times 10^5$, $\alpha = 0.98$, and $2r_0 = 1.36$ mm.

Coulomb gas in atomic physics

1) Gas of ionized atoms:
usually singly-ionized alkali-earth metals
(e.g. Berillium, Calcium, Magnesium).
Radiation is absorbed and emitted in the visible.

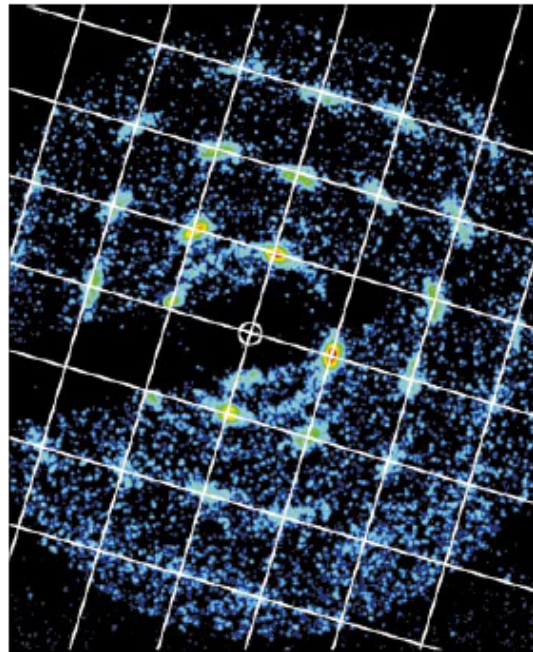
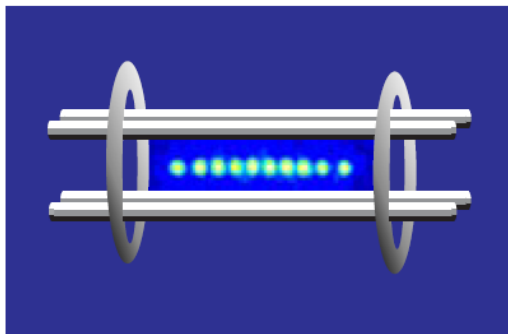


Fig. 4. Time-resolved Bragg diffraction pattern of the same plasma as in Fig. 2. Here and in Figs. 5

Coulomb gas in atomic physics

1) Gas of ionized atoms:
usually singly-ionized alkali-earth metals.
Radiation is absorbed and emitted in the visible.

2) Confinement by external potentials:
Paul (radiofrequency) or Penning traps.



Innsbruck Ion trap

Linear Paul trap:

$$\Phi_0 = U_{\text{dc}} + V_{\text{ac}} \cos(\Omega_{\text{rf}} t)$$

Effective harmonic force $\mathbf{F} \propto -\mathbf{r}$

Possibility to control the number of ions and the shape of the cloud

Coulomb gas in atomic physics

1) Gas of ionized atoms:

usually singly-ionized alkali-earth metals.

Radiation is absorbed and emitted in the visible.

2) Confinement by external potentials:

Paul (radiofrequency) or Penning traps.

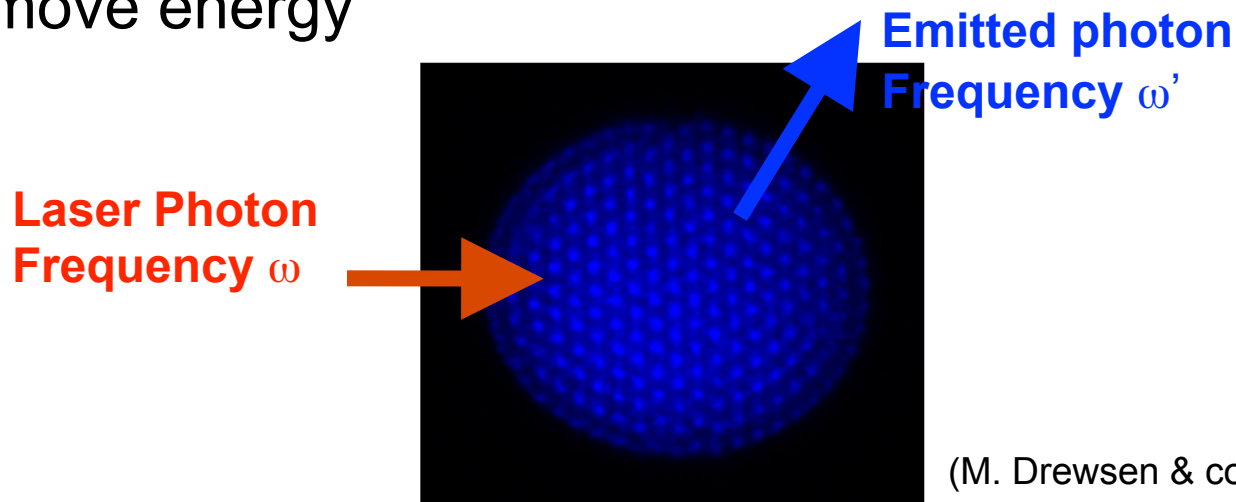
3) Crystallization:

Low thermal energies are achieved by laser cooling.

Cooling down to *few microKelvin*.

Crystallization: cooling via lasers

Radiation and matter exchange energy and momentum
Cooling: enhancement of photon-scattering processes
which remove energy



(M. Drewsen & coworkers, Aarhus)

$\omega < \omega'$: energy is transferred from the crystal to the photons
Cooling down to *few microKelvin*.

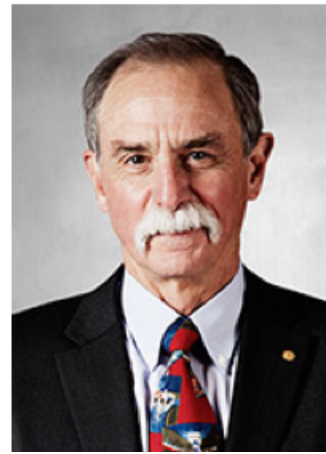
Trapped ions and Nobel Foundation



Dehmelt (1989)



Paul (1989)



Wineland (2012)

The Nobel Prize in Physics 1989 was divided, one half awarded to Norman F. Ramsey *"for the invention of the separated oscillatory fields method and its use in the hydrogen maser and other atomic clocks"*, the other half jointly to Hans G. Dehmelt and Wolfgang Paul *"for the development of the ion trap technique"*.

The Nobel Prize in Physics 2012 was awarded jointly to Serge Haroche and David J. Wineland *"for groundbreaking experimental methods that enable measuring and manipulation of individual quantum systems"*

And also: **Ramsey (1989), Chu, Cohen-Tannoudji, Phillips (1997), Haroche (2012)**

Crystals of ions in traps: Applications

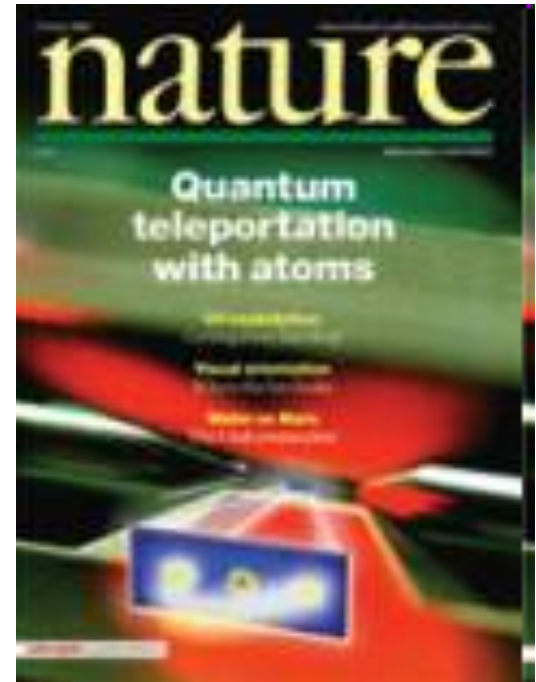
High-precision measurements

Simulation of astrophysical systems

Ultracold chemistry

Quantum-based technologies

Quantum simulators, quantum metrology,
Quantum computing.



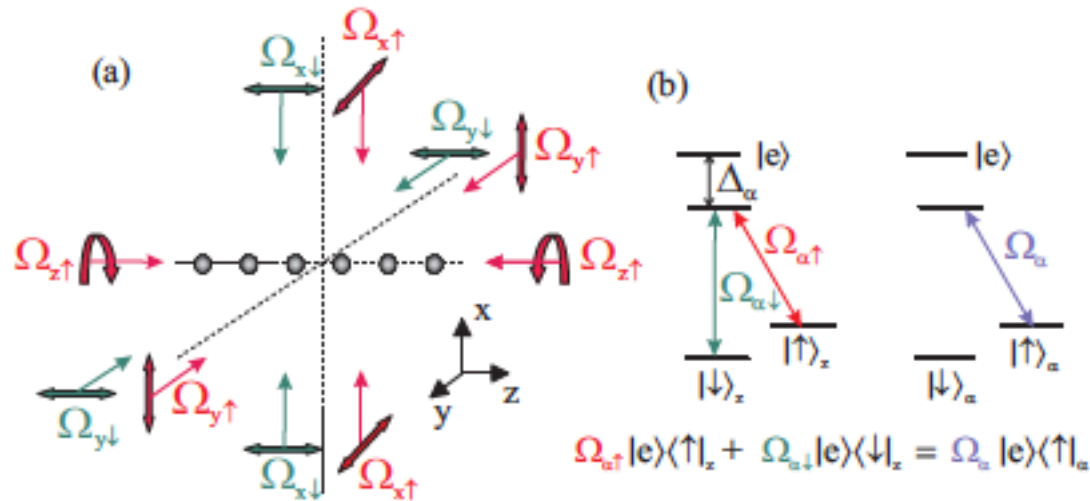
Aarhus, Berkeley, Boulder, Freiburg, Erlangen, Innsbruck, London, Mainz, Marseille, Michigan, München, Oxford, Paris, PTB, Saarbrücken, Siegen, Sussex,

Cirac, Zoller, Retzker, Plenio, Altman, Porras, Solano, Duan, ...

Engineering long-range interactions with trapped ions

Based on engineering the coupling between phonons and spins (Wunderlich, Porras, Cirac, Plenio, Retzker, Solano, Zoller...)

$$H_S^{XY} = \frac{1}{2} \sum_{i,j} (J_{i,j}^{[x]} \sigma_i^z \sigma_j^z + J_{i,j}^{[y]} \sigma_i^y \sigma_j^y) + \sum_i B^x \sigma_i^x$$



Engineering long-range interactions with trapped ions



Based on engineering the coupling between phonons and spins
(Wunderlich, Porras, Cirac, Plenio, Retzker, Solano,...)

Experiments:

Blatt, Bollinger, Monroe, Schätz, Wineland, Wunderlich

....

Picture: Chris Monroe's group

What about the system itself?

Negative Poisson's Ratios for Extreme States of Matter

Ray H. Baughman,^{1*} Socrates O. Dantas,² Sven Stafström,³
Anvar A. Zakhidov,¹ Travis B. Mitchell,⁴ Daniel H. E. Dubin⁵

Negative Poisson's ratios are predicted for body-centered-cubic phases that likely exist in white dwarf cores and neutron star outer crusts, as well as those found for vacuumlike ion crystals, plasma dust crystals, and colloidal crystals (including certain virus crystals). The existence of this counterintuitive property, which means that a material laterally expands when stretched, is experimentally demonstrated for very low density crystals of trapped ions. At very high densities, the large predicted negative and positive Poisson's ratios might be important for understanding the asteroseismology of neutron stars and white dwarfs and the effect of stellar stresses on nuclear reaction rates. Giant Poisson's ratios are both predicted and observed for highly strained coulombic photonic crystals, suggesting possible applications of large, tunable Poisson's ratios for photonic crystal devices.

Outline

- An unusual form of condensed matter
- Structural transitions: platform for studying criticality
- Novel paradigm of friction

**Ion chains: an unusual
form of condensed matter**

Low dimensional structures

VOLUME 68, NUMBER 13

PHYSICAL REVIEW LETTERS

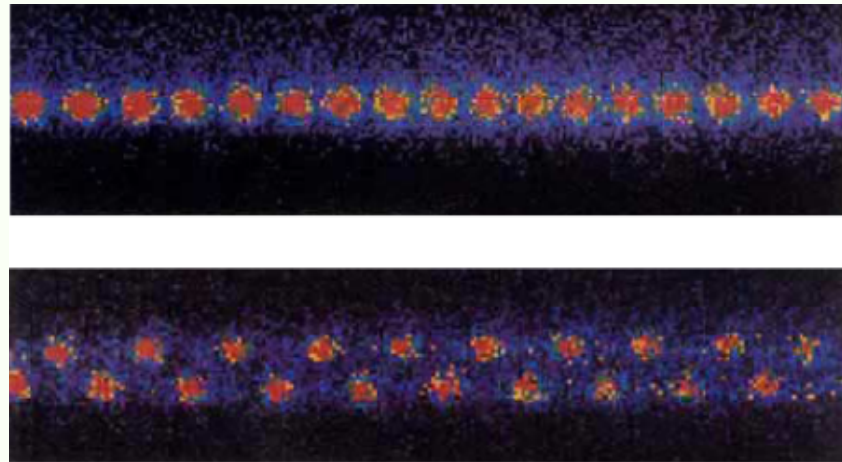
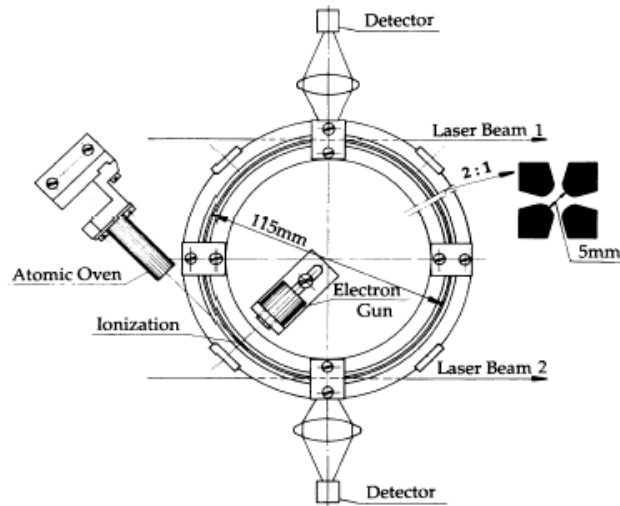
30 MARCH 1992

Observation of Ordered Structures of Laser-Cooled Ions in a Quadrupole Storage Ring

I. Waki,^(a) S. Kassner, G. Birkel, and H. Walther

Max-Planck-Institut für Quantenoptik, D-8046 Garching bei München, Federal Republic of Germany

(Received 11 September 1991; revised manuscript received 16 December 1991)



[Birkel et al., Nature 357, 310 (1992)]

The ion chain

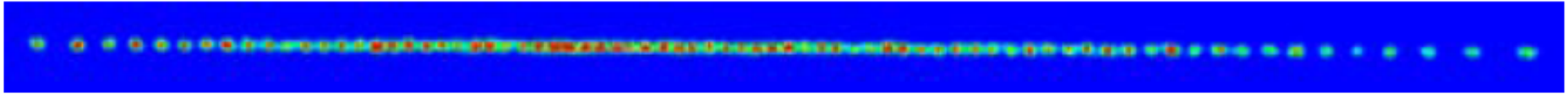
In textbooks (Ashcroft and Mermin):



Periodic distribution: Bloch theorem

Long-range interaction (Coulomb): no sound velocity

The ion chain in a linear trap



(M. Drewsen and coworkers, Aarhus)

$$H = \sum_{j=1}^N \frac{\mathbf{p}_j^2}{2m} + \frac{1}{2} m \left(\nu^2 x_j^2 + \nu_t^2 (y_j^2 + z_j^2) \right) + \frac{1}{2} \sum_{j=1}^N \sum_{i \neq j} \frac{Q^2}{r_{i,j}}$$

$\nu \ll \nu_t$ 1D structure (ion chain)

Inhomogeneous distribution: NO Bloch theorem

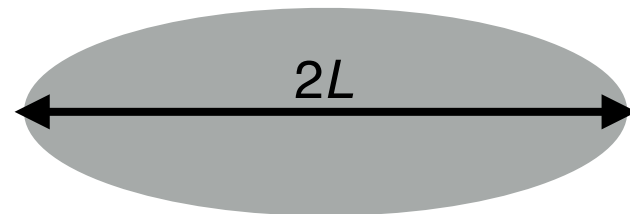
Long-range interaction:

perturbation theory with Bloch waves does not converge

Charge density at equilibrium

$$m\nu^2 x_i^{(0)} = - \sum_{j>i} \frac{Q^2}{(x_j^{(0)} - x_i^{(0)})^2} + \sum_{j<i} \frac{Q^2}{(x_i^{(0)} - x_j^{(0)})^2}$$

Naive continuum limit:
Apply Gauss theorem for a 3D
uniform cloud and project on 1D



Continuum limit: mean field description for 1D

Linear density:

$$n_L(x) = \frac{3}{4} \frac{N}{L} \left(1 - \frac{x^2}{L^2} \right)$$

Length of the chain:

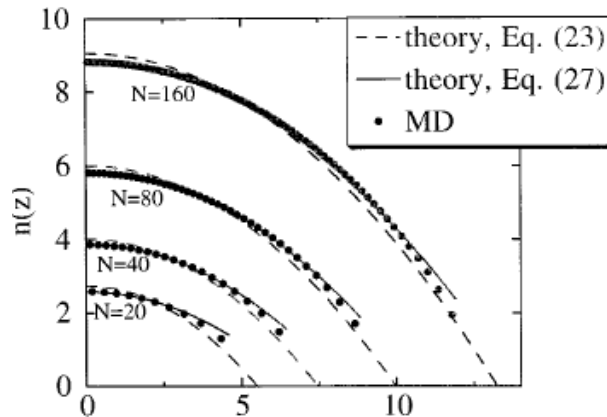
$$L(N)^3 = 3 \left(\frac{Q^2}{m\nu^2} \right) N \log N$$

at leading order in $1/\log N$

Charge density at equilibrium

$$m\nu^2 x_i^{(0)} = - \sum_{j>i} \frac{Q^2}{(x_j^{(0)} - x_i^{(0)})^2} + \sum_{j<i} \frac{Q^2}{(x_i^{(0)} - x_j^{(0)})^2}$$

Continuum limit: mean field description for 1D



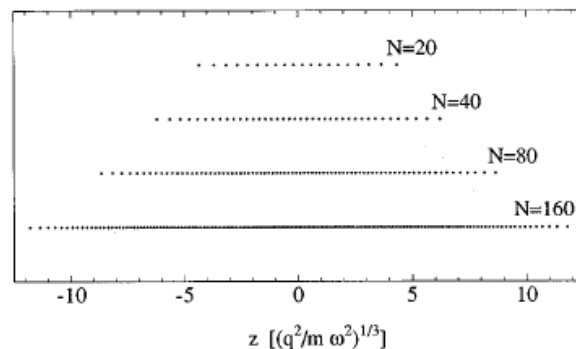
Linear density:

$$n_L(x) = \frac{3}{4} \frac{N}{L} \left(1 - \frac{x^2}{L^2} \right)$$

Length of the chain:

$$L(N)^3 = 3 \left(\frac{Q^2}{m\nu^2} \right) N \log N$$

at leading order in $1/\log N$



Harmonic vibrations around the equilibrium positions

$$q_i = x_i - x_i^{(0)}$$
$$\ddot{q}_i = -\nu^2 q_i - \sum_{j \neq i} \frac{K_{i,j}}{m} (q_i - q_j)$$
$$\ddot{y}_i = -\nu_t^2 y_i + \frac{1}{2} \sum_{j \neq i} \frac{K_{i,j}}{m} (y_i - y_j)$$
$$\ddot{z}_i = -\nu_t^2 z_i + \frac{1}{2} \sum_{j \neq i} \frac{K_{i,j}}{m} (z_i - z_j)$$
$$K_{i,j} = \frac{2Q^2}{|x_i^{(0)} - x_j^{(0)}|^3}$$

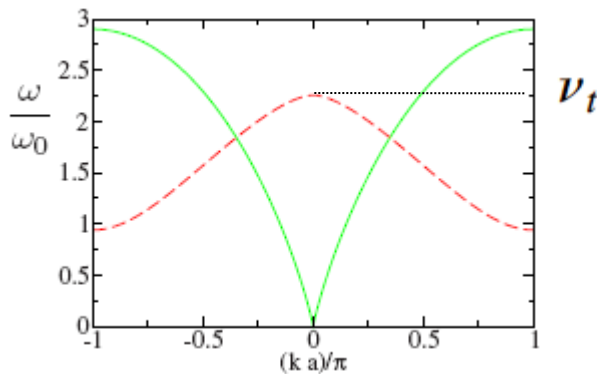
Fourier modes $\ddot{q}_i \longrightarrow -\omega^2 q_i$

Normal modes – Ring



No axial confinement: periodic distribution
Modes are phononic waves with quasimomentum k in BZ

Spectra of excitations



$$\omega_{\parallel}(k)^2 = 4 \left(\frac{2Q^2}{ma^3} \right) \sum_{j=1}^N \frac{1}{j^3} \sin^2 \frac{jka}{2}$$

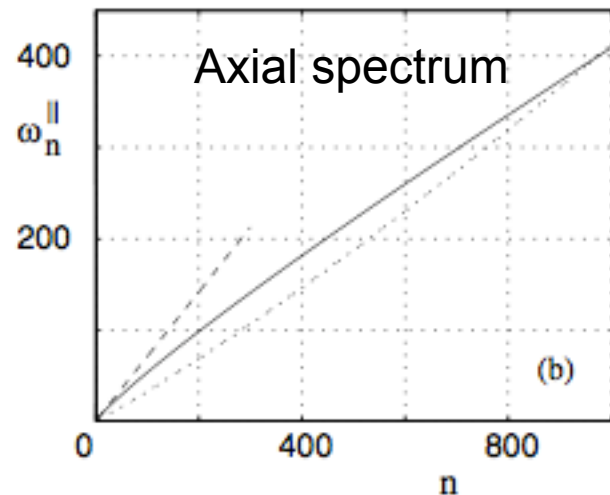
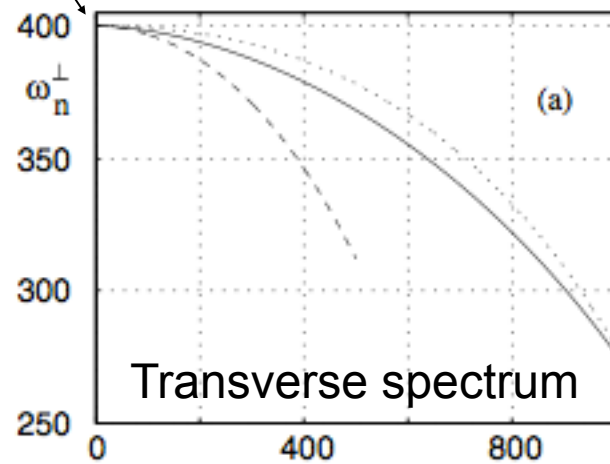
axial motion

$$\omega_{\perp}(k)^2 = \nu_t^2 - 2 \left(\frac{2Q^2}{ma^3} \right) \sum_{j=1}^N \frac{1}{j^3} \sin^2 \frac{jka}{2}$$

transverse motion

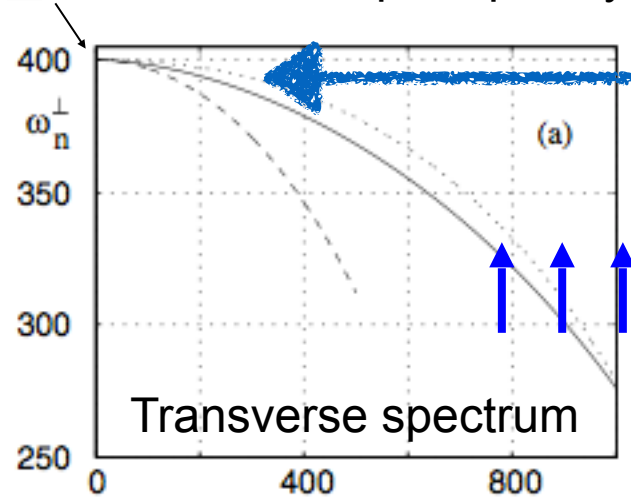
Trap: Spectra of excitations

ν_t Transverse trap frequency



Trap: Spectra of excitations

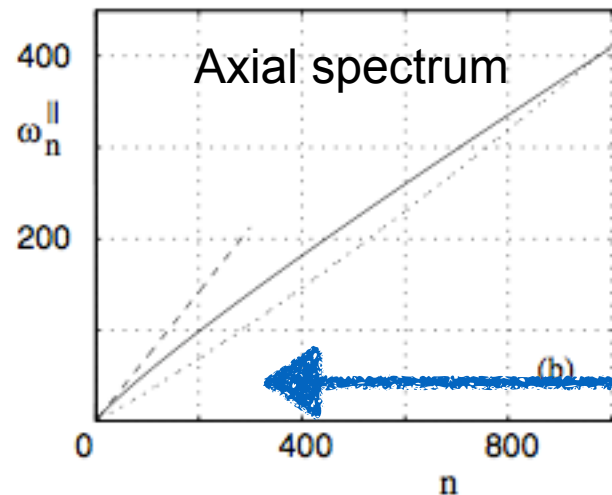
ν_t Transverse trap frequency



Long wavelength modes

Bulk mode $\omega_n^\perp = \nu_t$ $\uparrow \uparrow \uparrow \uparrow$

Stretch mode $\omega_n^\perp = \sqrt{\nu_t^2 - \nu^2}$ $\uparrow \uparrow \downarrow \downarrow$

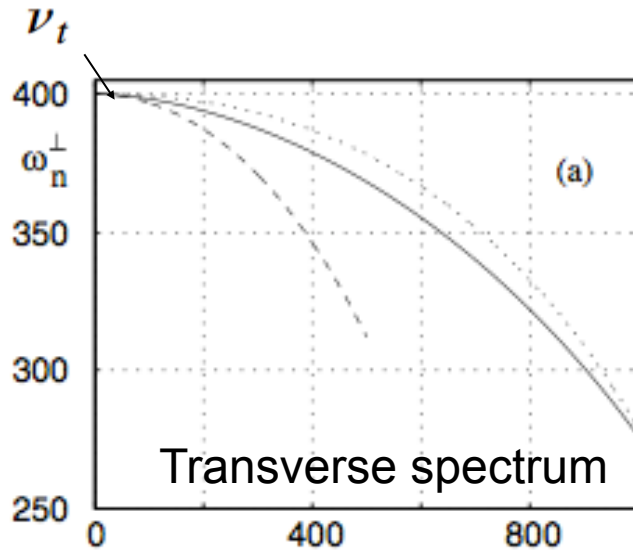


Bulk mode $\omega_n^\parallel = \nu$ $\rightarrow \rightarrow \rightarrow \rightarrow$

Stretch mode $\omega_n^\parallel = \sqrt{3}\nu$ $\rightarrow \rightarrow \leftarrow \leftarrow$

Long wavelength modes

Trap: Spectra of excitations

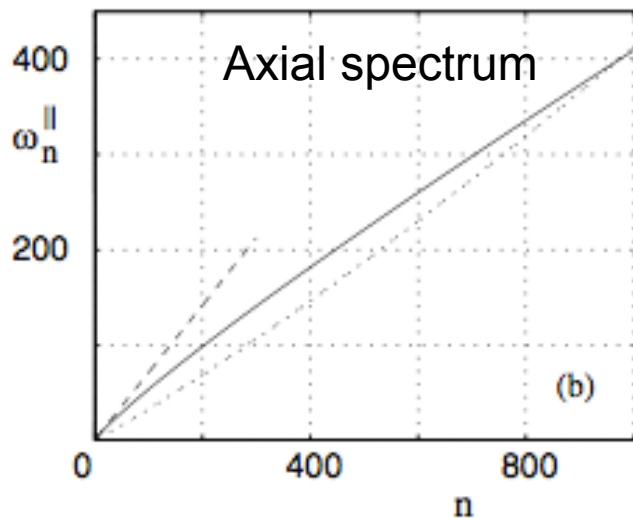


Transverse spectrum

Zigzag mode



Short wavelength modes



Axial spectrum

Short wavelength modes

Zigzag mode



Long-wavelength modes

$$(\omega^2 - \nu^2)q_i = \nu^2 \mathcal{K}_0 \sum_{i \neq j} \frac{1}{|\xi_i^{(0)} - \xi_j^{(0)}|^3} (q_i - q_j)$$

$$\mathcal{K}_0 = \frac{2Q^2}{m\nu^2 L(N)^3} = \frac{2}{3N \log N}$$

Equilibrium position $\xi_i^{(0)} = x_i^{(0)} / L$

Interparticle distance $a(\xi_i) = a_L(x_i) / L$

Linear density $n(\xi) = 1 - \xi^2$

Long-wavelength modes

$$(\omega^2 - \nu^2)q_i = \nu^2 \mathcal{K}_0 \sum_{j \neq i} \frac{1}{|\xi_i^{(0)} - \xi_j^{(0)}|^3} (q_i - q_j)$$

Continuum approximation (away from ends):

$$\begin{aligned} (\omega^2 - \nu^2)q(\xi) = & \frac{3}{4}\nu^2 \mathcal{K}_0 N \int_{-1}^{\xi - a(\xi)} d\xi' \frac{n(\xi')}{(\xi - \xi')^3} (q(\xi) - q(\xi')) \\ & + \int_{\xi + a(\xi)}^1 d\xi' \frac{n(\xi')}{(\xi' - \xi)^3} (q(\xi) - q(\xi')) \end{aligned}$$

Long-wavelength modes

Leading order in $1/\log N$ $(\omega^2 - \nu^2)q(\xi) = \frac{3}{4}\nu^2\mathcal{K}_0N I_0[\xi, w(\xi)]$

$$I_0[\xi, w(\xi)] \approx -\log N \boxed{(1 - \xi^2)w''(\xi) - 4\xi w'(\xi)}$$

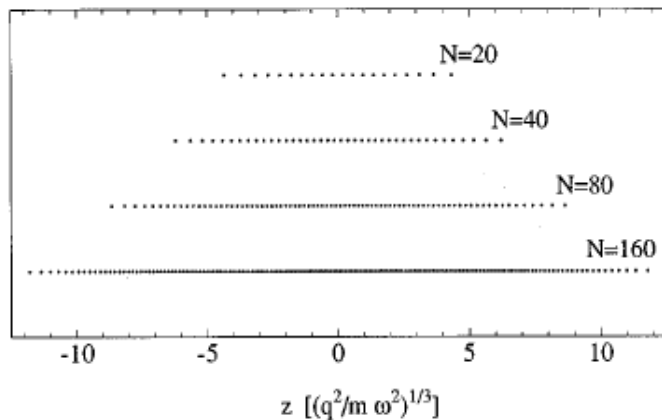
Jacobi Polynomials differential equation

Eigenmodes: $P_\ell^{1,1}(\bar{x})$

Axial Eigenfrequencies: $\omega_n^{\parallel \text{ Jac}} = \nu \sqrt{\frac{n(n+1)}{2}}$

Transverse Eigenfrequencies: $\omega_n^{\perp \text{ Jac}} = \sqrt{\nu_t^2 - \frac{(n-1)(n+2)}{4}}\nu^2$

Short-wavelength modes



They are localized at the chain center
(where the distance is smaller)

The distance in the chain center is
uniform

The short-wavelength modes are to good
approximation sinusoidal waves

demonstrate with phonon-like approximation

$$q_j = A_j e^{i(kja - \omega t)} \quad \text{slowly varying } A_j$$

Statistical Mechanics

Quantization of the vibrations

$$\hat{H}_n = \sum_{n=1}^N \hbar \omega_n^{\parallel} \hat{N}_n^{\parallel} + \sum_{n=1}^N \hbar \omega_n^{\perp} (\hat{N}_{n,y}^{\perp} + \hat{N}_{n,z}^{\perp})$$

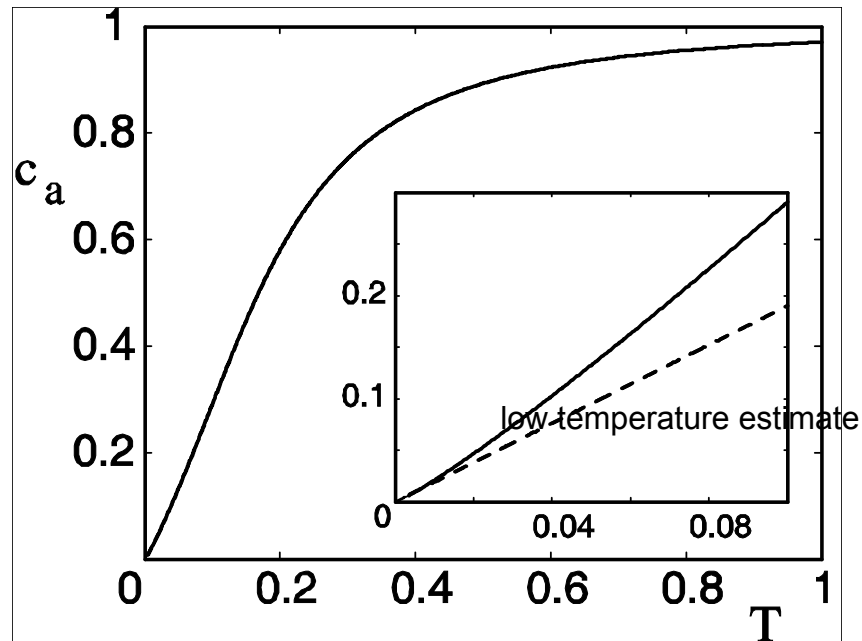
Canonical ensemble $\rho = \frac{1}{Z} \exp(-\beta H) \quad F = -k_B T \log Z$

One-dimensional behaviour: $k_B T \ll \hbar \omega_{\min}^{\perp}$

Thermodynamic limit: $\nu \sim \sqrt{\log N}/N$ as $N \rightarrow \infty$

Density in the center $n(0) = \frac{3}{4} \frac{N}{L}$ fixed

Specific Heat



Non extensive behaviour at low temperatures in the thermodynamic limit:

$$c_a \propto 1 / \sqrt{\ln N}$$

- Due to long-range Coulomb interaction
- It is a quantum effect (at high- T Dulong-Petit holds)

Equivalence of ensembles

$$\text{Relative energy fluctuation} \propto \frac{1}{\sqrt{C_a}} = \left(\frac{\sqrt{\ln N}}{N} \right)^{1/2}$$

Validity of the assumption of a Canonical ensemble

Ions are laser cooled (thermal distribution?)

Thermalization by collisions:
the $N-1$ ions are a reservoir for each ion in the chain

Role of anharmonicities?
(Fermi-Pasta-Ulam paradigm)

Statistical mechanics of a chain of oscillators?

Ion chains as thermal reservoirs?

- In the *harmonic* chain the dynamics is integrable

JOURNAL OF MATHEMATICAL PHYSICS

VOLUME 6, NUMBER 4

APRIL 1965

Statistical Mechanics of Assemblies of Coupled Oscillators*

G. W. FORD†

Department of Physics, University of Michigan, Ann Arbor, Michigan

M. KAC

The Rockefeller Institute, New York, New York

AND

P. MAZUR

Lorentz Institute for Theoretical Physics, Leiden, The Netherlands

(Received 25 September 1964)

It is shown that a system of coupled harmonic oscillators can be made a model of a heat bath. Thus a particle coupled harmonically to the bath and by an arbitrary force to a fixed center will (in an appropriate limit) exhibit Brownian motion. Both classical and quantum mechanical treatments are given.

- The rest of the chain acts as a bath for a single ion (when thermalization rate is faster than recurrence)

Thermalization and entanglement

Effective dynamics of one ion

Langevin equation:

$$\frac{d^2 X_{\pm}}{dt^2} + \boxed{\int_0^t \Gamma_{\pm}(t-t') \frac{dX_{\pm}}{dt'} dt'} + (1 - \Gamma_{\pm}(0))X_{\pm}(t) = F_{\pm}(t) - \Gamma_{\pm}(t)X_{\pm}(0)$$

damping kernel

Spectral density (Fourier transform of the damping kernel)

$$J_{\pm}(\omega) = \omega \int_0^{\infty} \Gamma_{\pm}(t) \cos(\omega t) dt$$

Effective dynamics of one ion

Langevin equation:

$$\frac{d^2 X_{\pm}}{dt^2} + \boxed{\int_0^t \Gamma_{\pm}(t-t') \frac{dX_{\pm}}{dt'} dt'} + (1 - \Gamma_{\pm}(0))X_{\pm}(t) = F_{\pm}(t) - \Gamma_{\pm}(t)X_{\pm}(0)$$

damping kernel

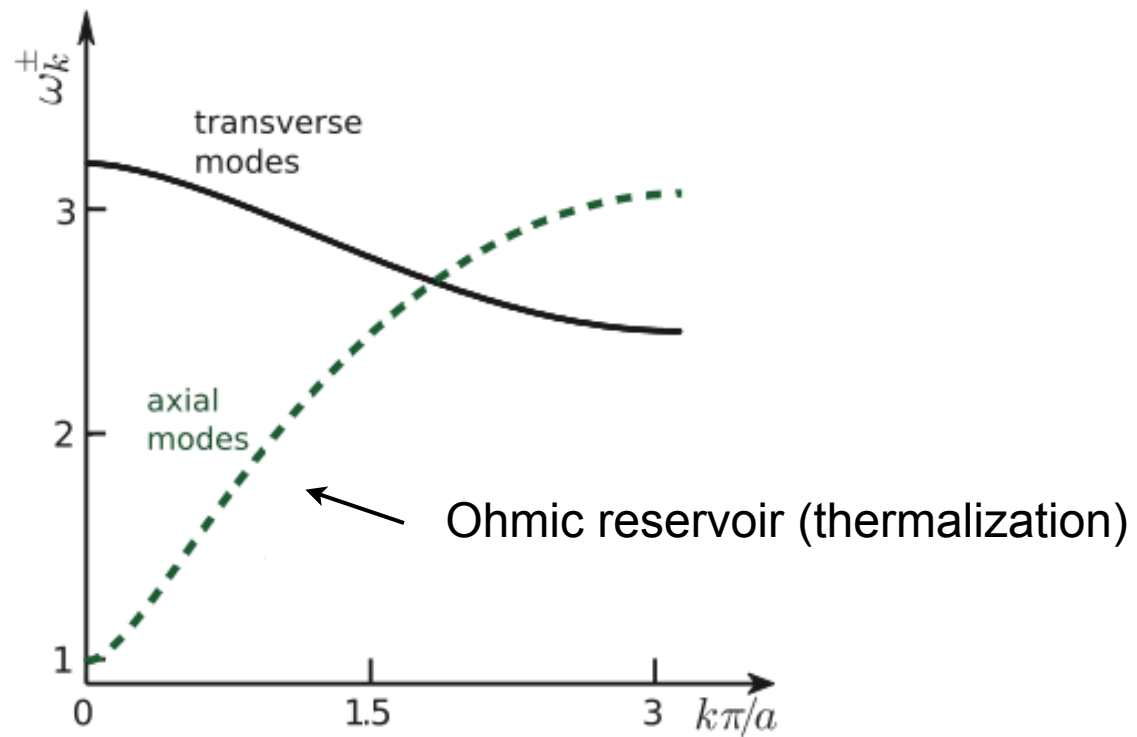
Spectral density (Fourier transform of the damping kernel)

$$J_{\pm}(\omega) = \omega \int_0^{\infty} \Gamma_{\pm}(t) \cos(\omega t) dt$$

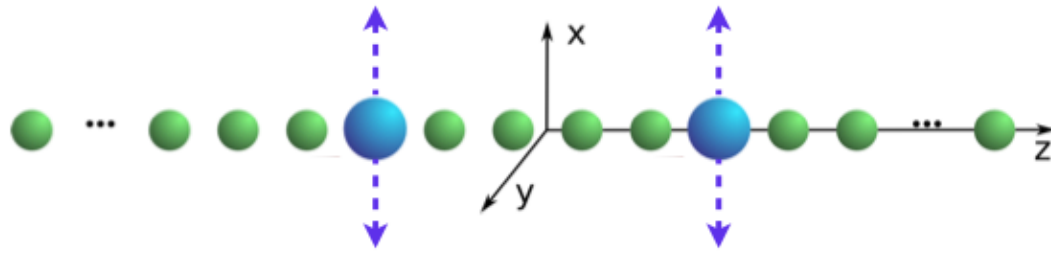
Its properties are determined by the excitation spectrum of the chain:

$$J(\omega) = \frac{\pi}{2m} \sum_{i=-N}^N \frac{\bar{\gamma}_i^2}{\bar{\omega}_i} \delta(\omega - \bar{\omega}_i)$$

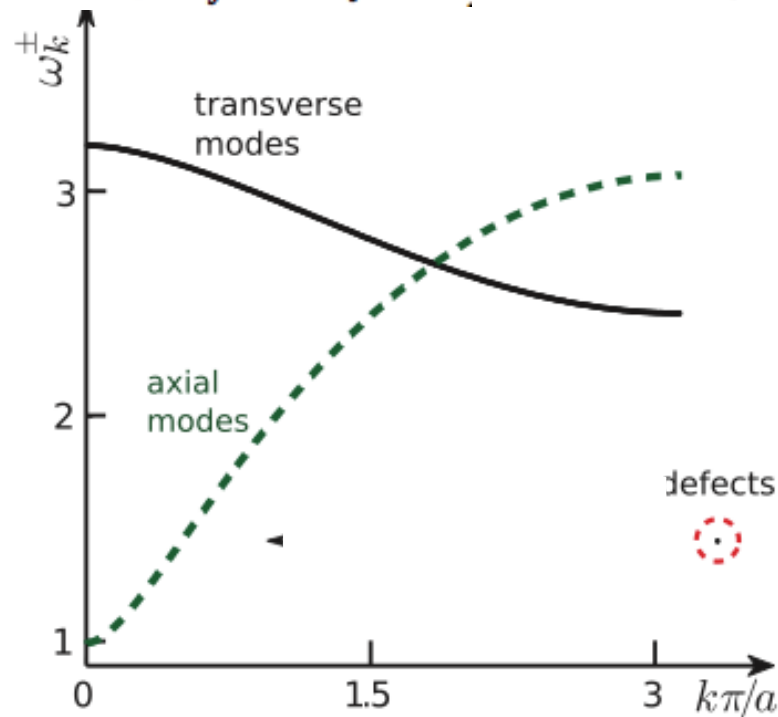
Spectral properties (reminder)



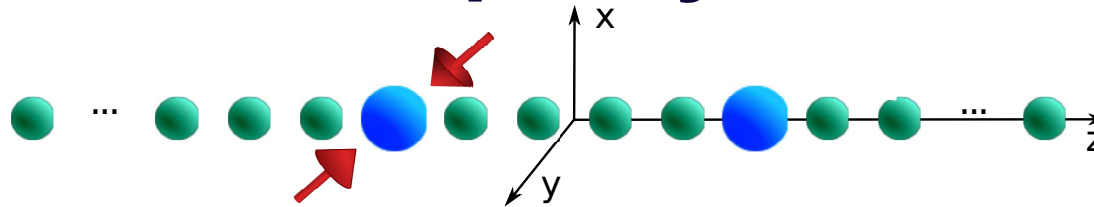
Engineering the spectral properties



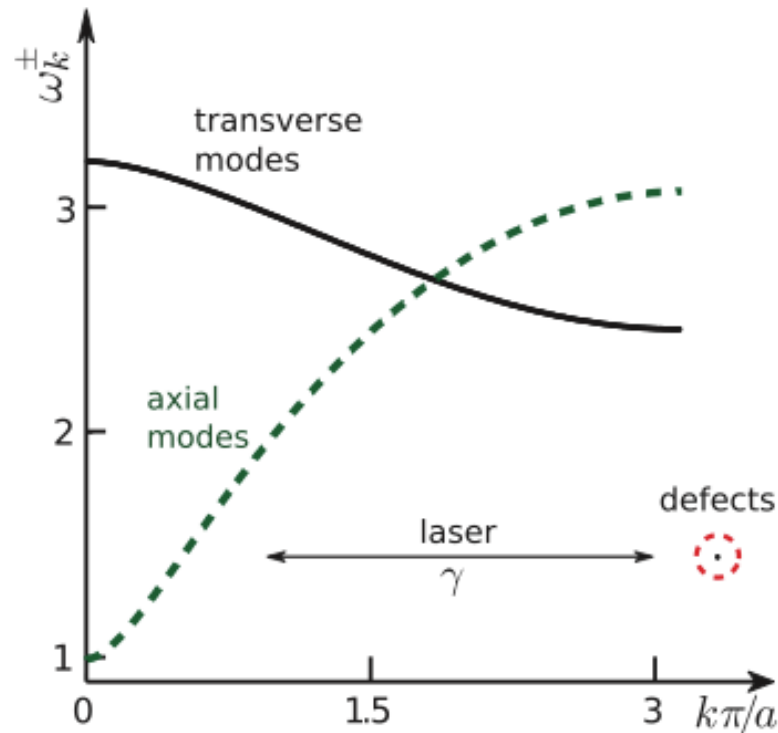
$$V_{\text{trap}}(\mathbf{r}_j) = [U_{\parallel} z_j^2 + U_{\perp,j}(x_j^2 + y_j^2)]/2 \quad \text{and} \quad U_{\perp,j} = (U_0/m_j - U_{\parallel})/2$$



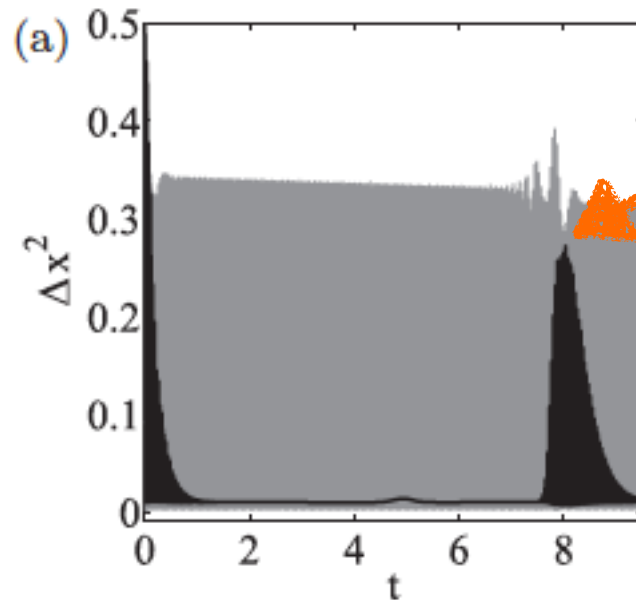
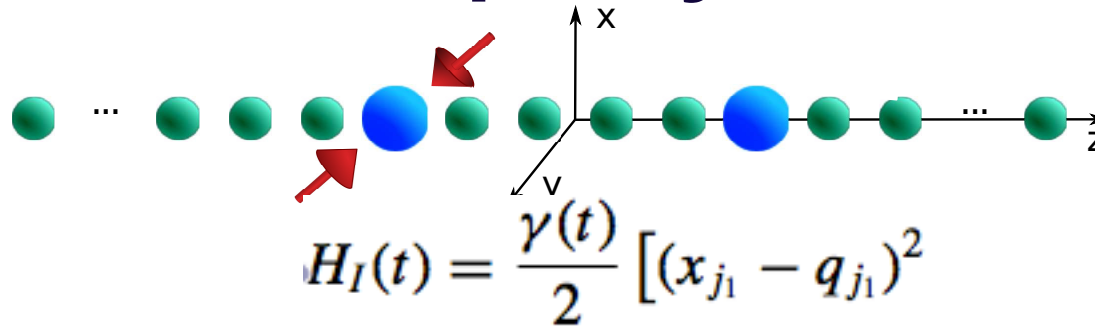
Thermalization of one impurity defect?



$$H_I(t) = \frac{\gamma(t)}{2} (x_{j_1} - q_{j_1})^2$$



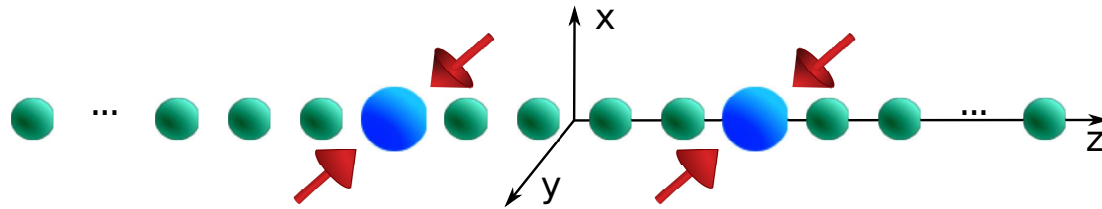
Thermalization of one impurity defect .



Revival time

Thermalization occurs for any initial state.
The rate scales with the coupling strength

What about two impurity defects?



$$H_I(t) = \frac{\gamma(t)}{2} [(x_{j_1} - q_{j_1})^2 + (x_{j_2} - q_{j_2})^2]$$

About stationary quantum correlations

PHYSICAL REVIEW A **66**, 042327 (2002)

Entanglement properties of the harmonic chain

K. Audenaert,^{*} J. Eisert,[†] and M. B. Plenio[‡]

QOLS, Blackett Laboratory, Imperial College of Science, Technology and Medicine, London SW7 2BW, United Kingdom

R. F. Werner [§]

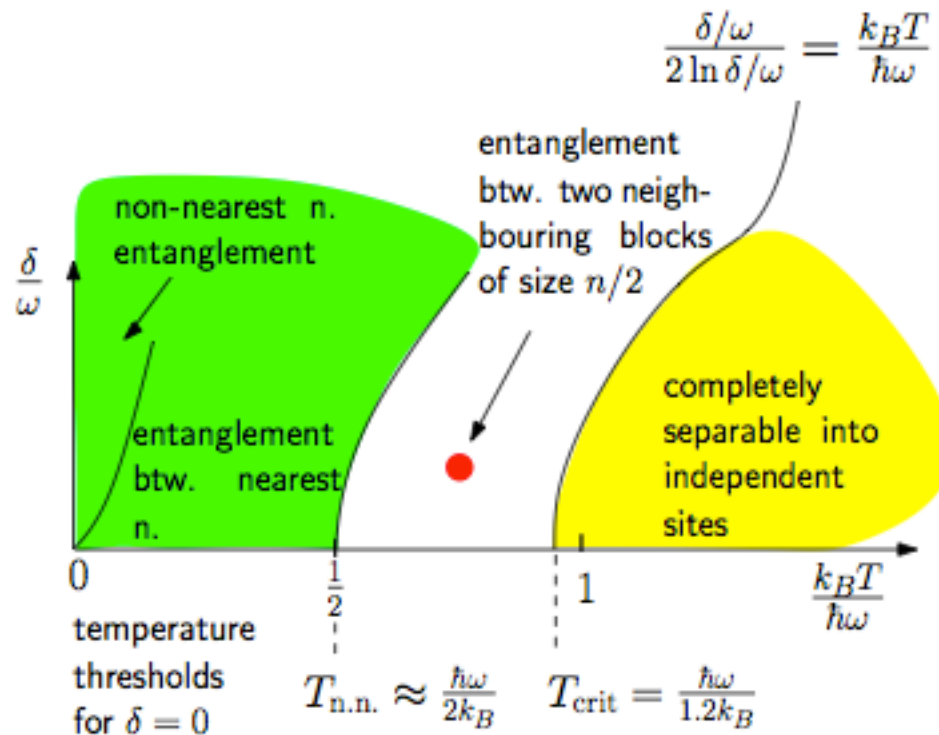
Institut für Mathematische Physik, TU Braunschweig, Mendelssohnstraße 3, 38106 Braunschweig, Germany

(Received 14 May 2002; published 30 October 2002)

Stationary quantum correlations II

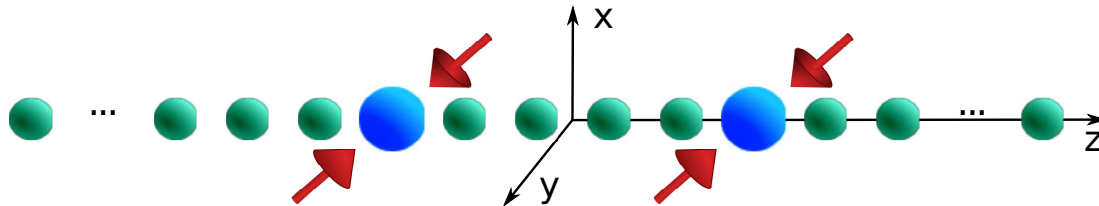
Entanglement and separability of quantum harmonic oscillator systems at finite temperature

Janet Anders¹ and Andreas Winter^{1,2}



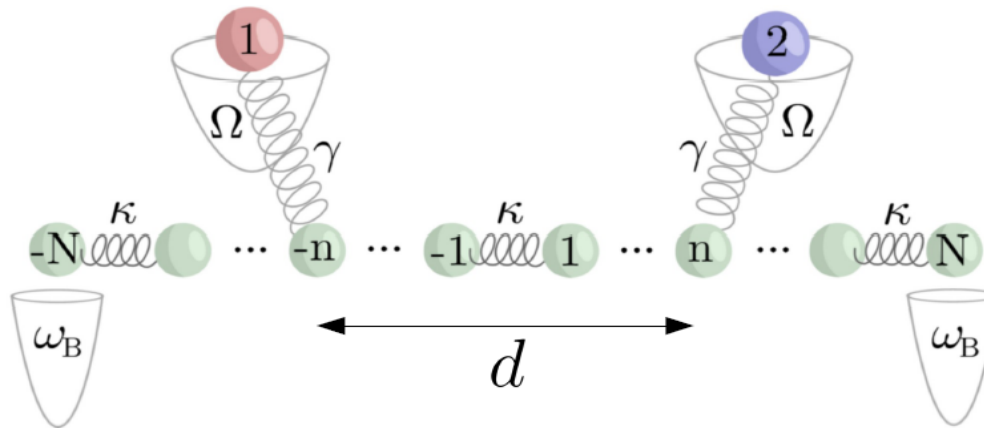
Entanglement & Symmetries

- Chain with periodic boundary conditions: Discrete translational invariance, no entanglement beyond nearest-neighbours.
- Impurity defects: discrete translational invariance is broken. Symmetry per reflection



- Symmetry: Decoherence Free Subspaces?

Symmetries

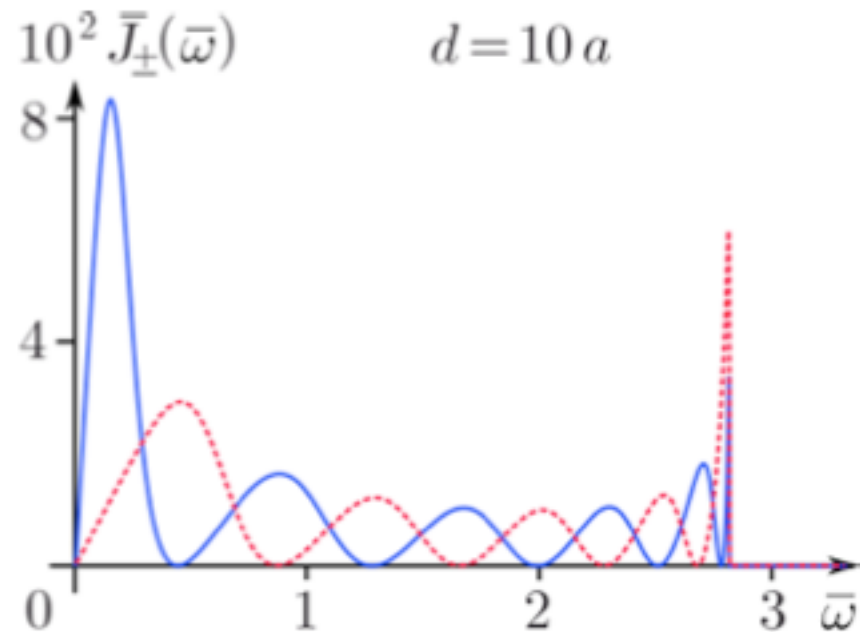
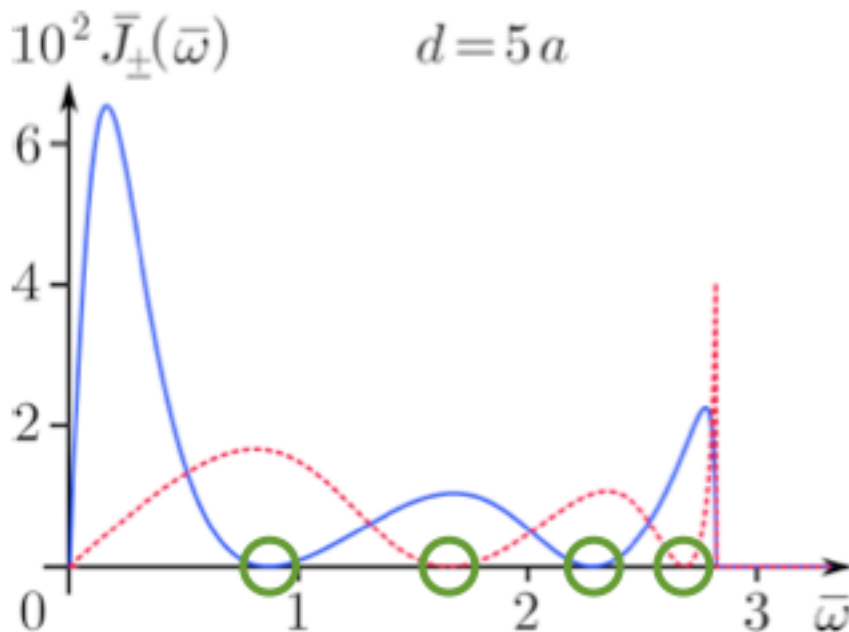
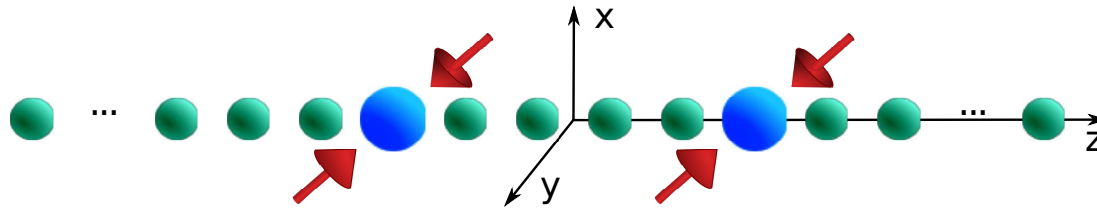


Center-of-mass and relative coordinates

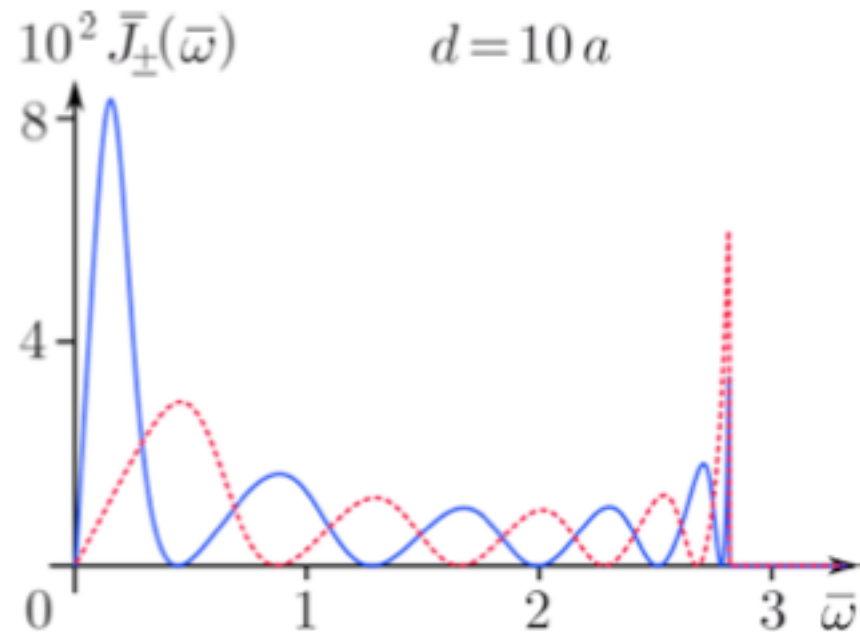
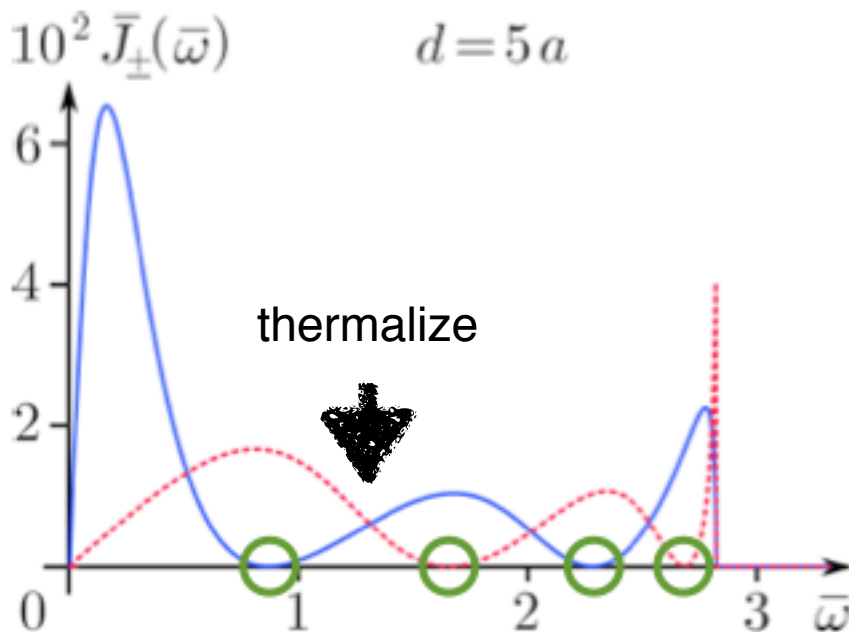
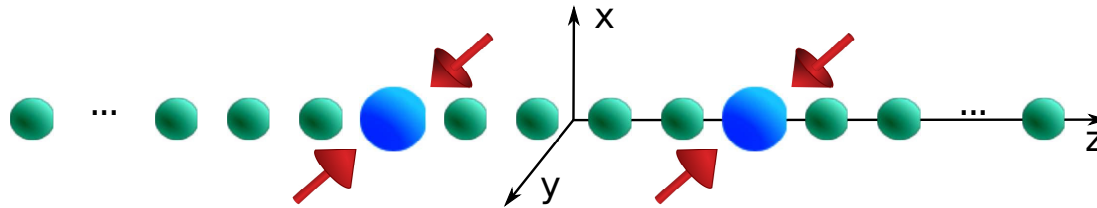
$$X_{\pm} = (X_1 \pm X_2)/\sqrt{2} \quad \text{Defects}$$

$$x_i^{\pm} = (x_{-i} \pm x_i)/\sqrt{2} \quad \text{Bulk ions}$$

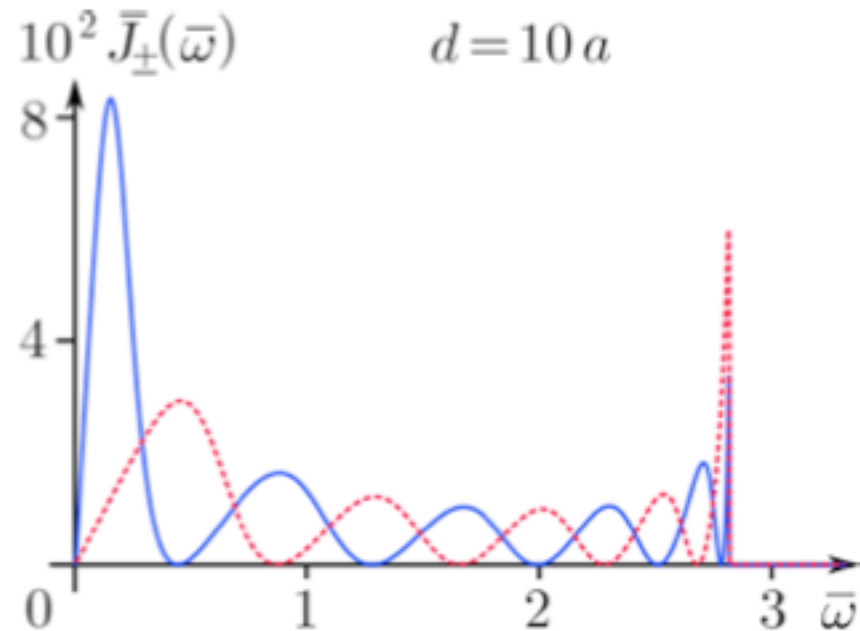
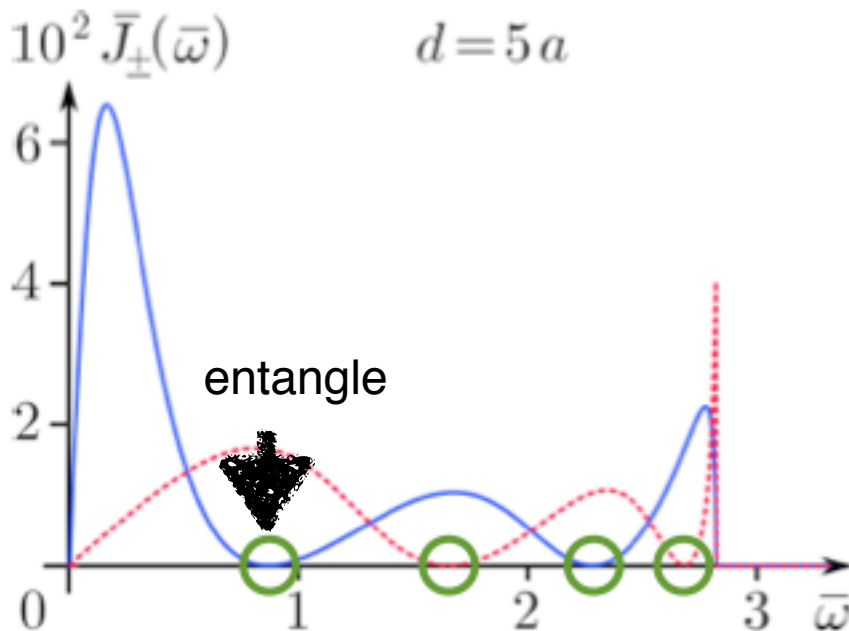
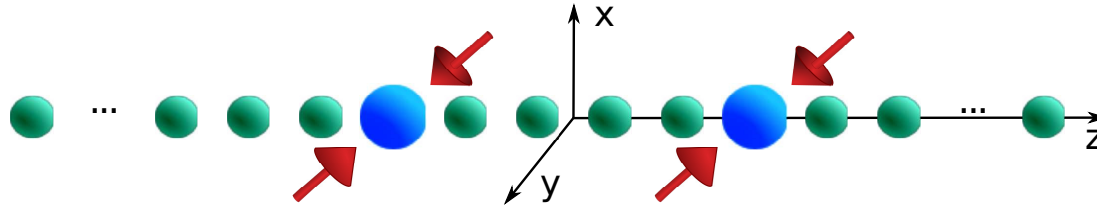
Spectral density for distant defects



Spectral density for distant defects



Spectral density for distant defects



changing the frequency of the defects: switch the bath from Markovian to non-Markovian.

Thermalization “generates” entanglement

Covariance matrix for the two impurities (t=0)

$$\bar{\Sigma}(0) = \begin{pmatrix} \bar{\sigma}_{-n}(0) & 0 \\ 0 & \bar{\sigma}_n(0) \end{pmatrix}$$

Thermalization “generates” entanglement

$$\bar{\Sigma}(0) = \begin{pmatrix} \bar{\sigma}_{-n}(0) & 0 \\ 0 & \bar{\sigma}_n(0) \end{pmatrix} \rightarrow \frac{1}{2} \begin{pmatrix} \bar{\sigma}_{-n}(0) + \bar{\sigma}_n(0) & \bar{\sigma}_{-n}(0) - \bar{\sigma}_n(0) \\ \bar{\sigma}_{-n}(0) - \bar{\sigma}_n(0) & \bar{\sigma}_{-n}(0) + \bar{\sigma}_n(0) \end{pmatrix}$$

In terms of COM and relative motion (t=0)

Thermalization “generates” entanglement

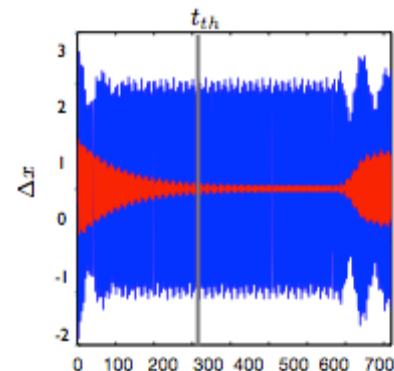
$$\bar{\Sigma}(0) = \begin{pmatrix} \bar{\sigma}_{-n}(0) & 0 \\ 0 & \bar{\sigma}_n(0) \end{pmatrix} \rightarrow \frac{1}{2} \begin{pmatrix} \bar{\sigma}_{-n}(0) + \bar{\sigma}_n(0) & \bar{\sigma}_{-n}(0) - \bar{\sigma}_n(0) \\ \bar{\sigma}_{-n}(0) - \bar{\sigma}_n(0) & \bar{\sigma}_{-n}(0) + \bar{\sigma}_n(0) \end{pmatrix}$$

Time evolution thermalizes relative motion



$$\begin{pmatrix} \bar{\sigma}^+(t > t_{th}) & 0 \\ 0 & \bar{\sigma}^-(T) \end{pmatrix}$$

COM
REL



Thermalization “generates” entanglement

$$\bar{\Sigma}(0) = \begin{pmatrix} \bar{\sigma}_{-n}(0) & 0 \\ 0 & \bar{\sigma}_n(0) \end{pmatrix} \rightarrow \frac{1}{2} \begin{pmatrix} \bar{\sigma}_{-n}(0) + \bar{\sigma}_n(0) & \bar{\sigma}_{-n}(0) - \bar{\sigma}_n(0) \\ \bar{\sigma}_{-n}(0) - \bar{\sigma}_n(0) & \bar{\sigma}_{-n}(0) + \bar{\sigma}_n(0) \end{pmatrix}$$



**Cross-correlations
between the defects**

$$\begin{pmatrix} \bar{\sigma}^+(t > t_{th}) & 0 \\ 0 & \bar{\sigma}^-(T) \end{pmatrix}$$



$$\bar{\Sigma}(t > t_{th}) = \frac{1}{2} \begin{pmatrix} \bar{\sigma}^+(t) + \bar{\sigma}^-(T) & \bar{\sigma}^+(t) - \bar{\sigma}^-(T) \\ \bar{\sigma}^+(t) - \bar{\sigma}^-(T) & \bar{\sigma}^+(t) + \bar{\sigma}^-(T) \end{pmatrix}$$

cross correlations can be quantum

Entanglement is **two-mode squeezing (EPR)**

- Initially squeezed defects: The COM is squeezed (**s**)
- Relative motion is thermalized (**T**)
- Large **s** and low **T**: the two orthogonal quadratures are below the standard quantum limit

$$C_{1,2}(t) = 1 - \frac{2\langle Q_1(t, \theta_1) Q_2(t, \theta_2) \rangle}{\langle Q_1(t, \theta_1)^2 \rangle + \langle Q_2(t, \theta_2)^2 \rangle} < 1$$

Logarithmic negativity

$$C_{1,2}(t) = 1 - \frac{2\langle Q_1(t, \theta_1) Q_2(t, \theta_2) \rangle}{\langle Q_1(t, \theta_1)^2 \rangle + \langle Q_2(t, \theta_2)^2 \rangle} < 1$$

We analyse entanglement from the partial transpose of the covariance matrix

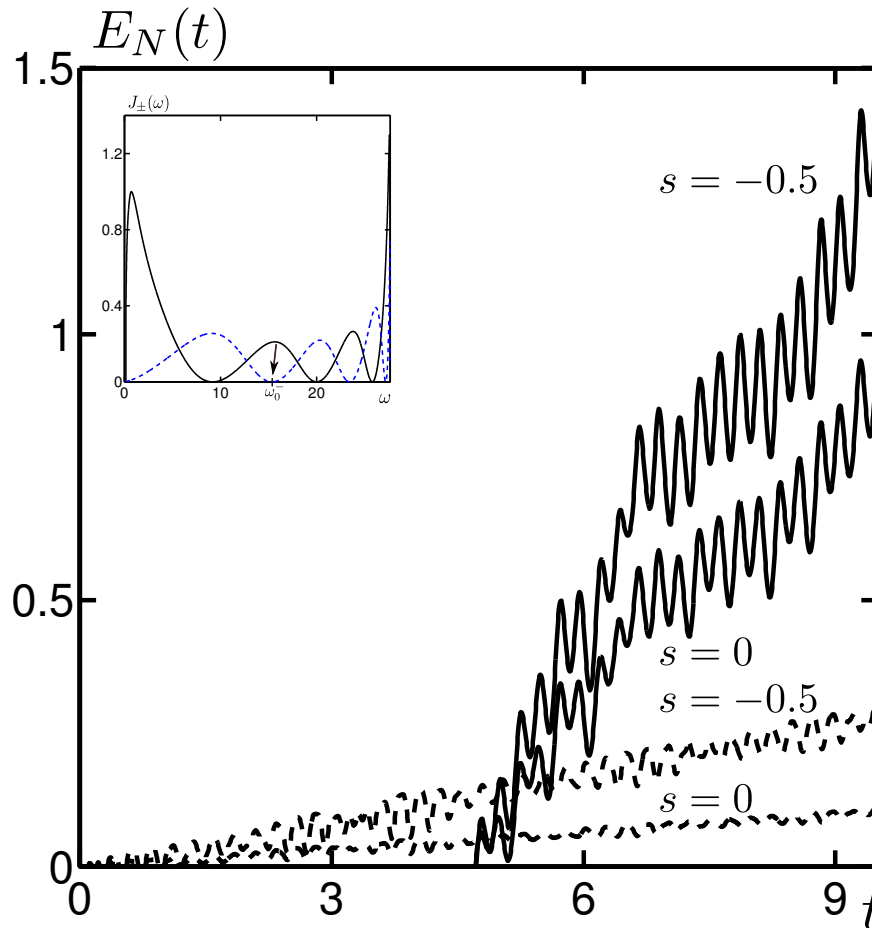
$$\Sigma_{ij} = \frac{1}{2} \langle \xi_i \xi_j + \xi_j \xi_i \rangle - \langle \xi_i \rangle \langle \xi_j \rangle$$

$$\xi = (q_{j1}, \bar{p}_{j1,q}, q_{j2}, p_{j2,q})$$

using the logarithmic negativity

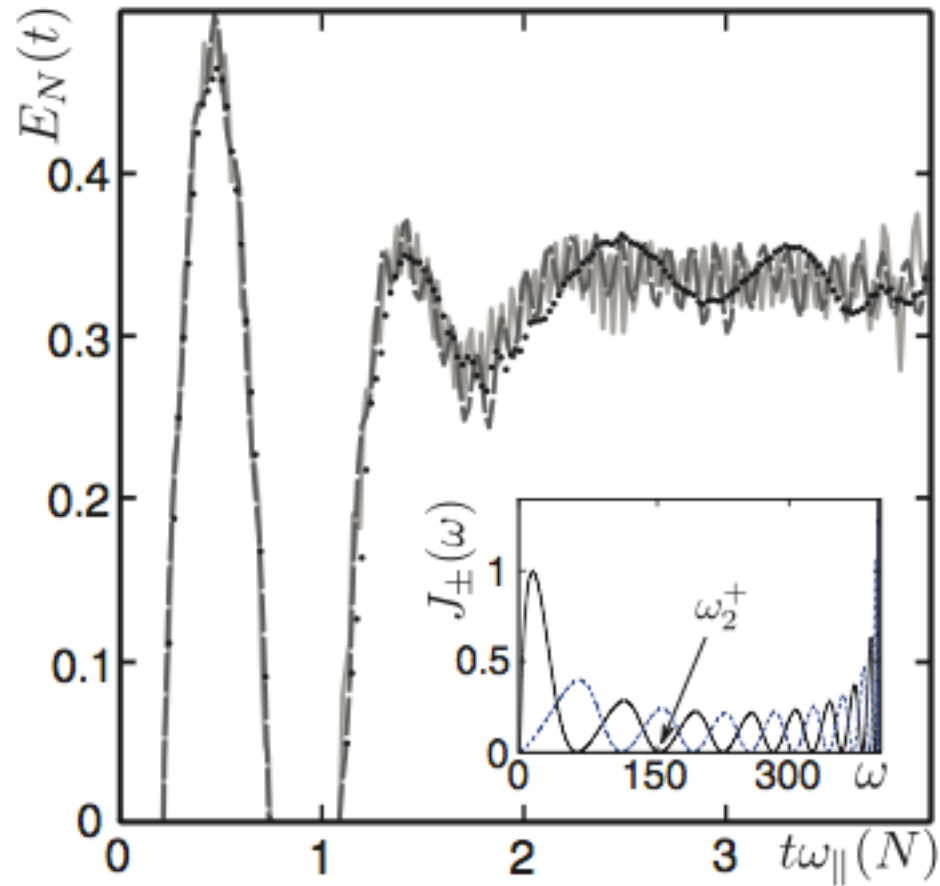
$$E_N = \max\{0, -\ln(2\tilde{v}_-)\}$$

Dynamics of Entanglement



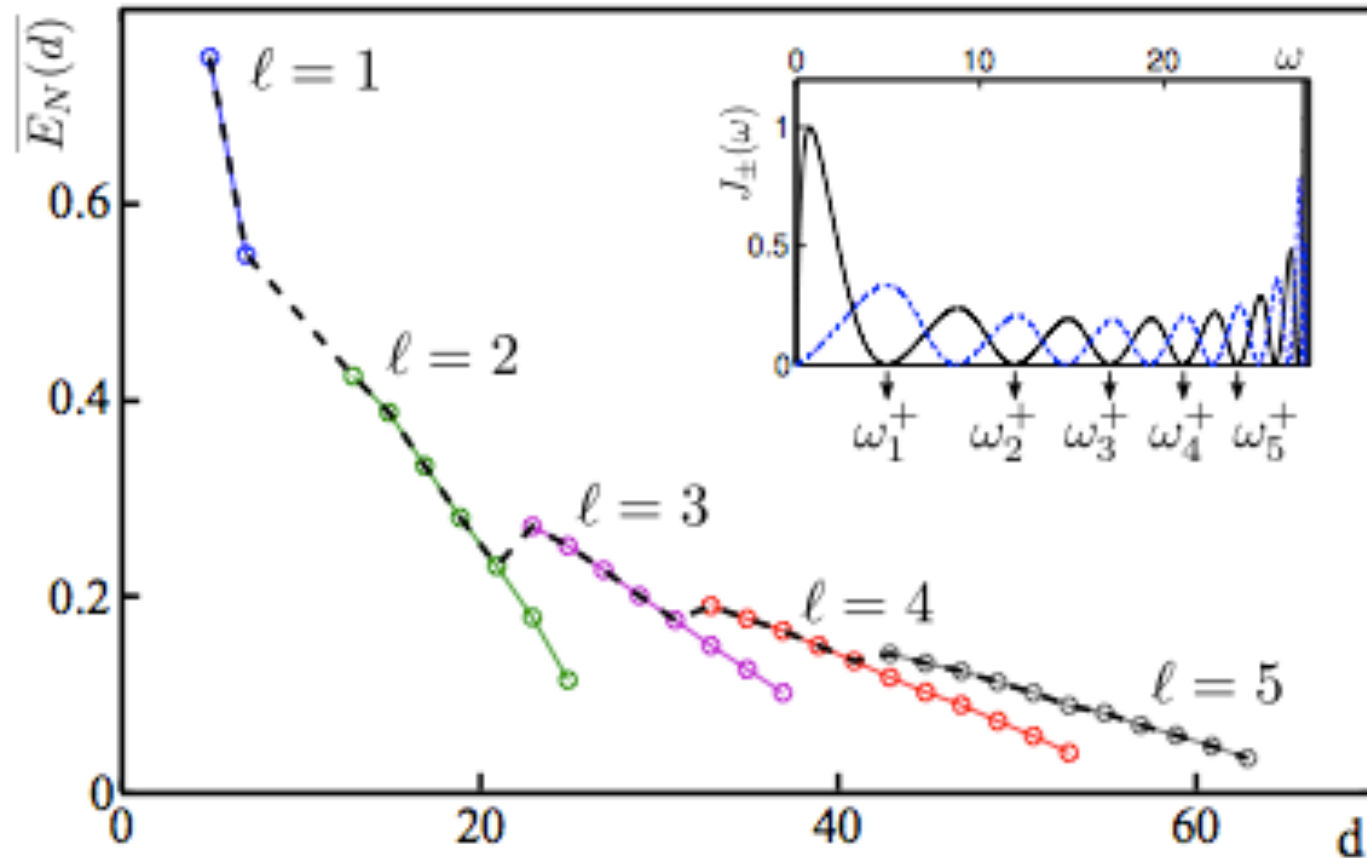
distance $d=5a$, chain of 50 ions in a thermal state
(ions: Calcium, impurity defects: Indium).

Scaling with the number of ions



Curves for $N=800, 1000, 1200$ ions

Scaling with the distance



slow decay with the distance

Detection

Perform tomography of the defects density matrix by
locally coupling spin and mode

$$H_{i=1,2}^{\text{int}} = g_i(t) \sigma_i^z (a_i e^{-i\Omega_i t} + a_i^\dagger e^{i\Omega_i t})$$

measuring

$$\langle T \rangle = \langle \sigma^x \otimes \sigma^x - \sigma^y \otimes \sigma^y + i\sigma^x \otimes \sigma^y + i\sigma^y \otimes \sigma^x \rangle$$

this gives access to

$$\begin{aligned} \chi_\rho(\alpha, \beta) &= \text{Tr}[\rho(t) D_{j_1}(\alpha) \otimes D_{j_2}(\beta)] \\ &= 4\langle T \rangle(t). \end{aligned}$$

where the coefficients can be varied by changing the pulse areas

Thanks to

S. Fishman



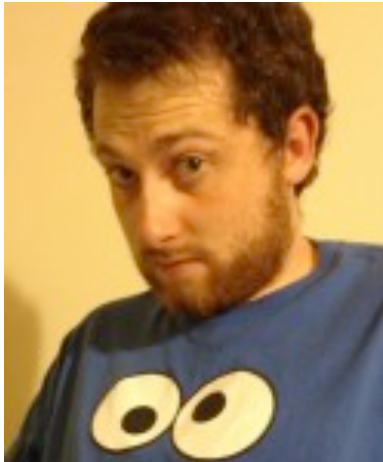
J. Baltrusch



Th. Busch



B. Taketani



T. Fogarty



E. Kajari



A. Wolf



E. Lutz

Some literature

G. Morigi and S. Fishman, Phys. Rev. Lett. 93, 170602 (2004).

G. Morigi and S. Fishman, Phys. Rev. E 70, 066141 (2004).

A.Wolf et al, Europhysics Letters 95, 60008 (2011).

E.Kajari et al, Phys. Rev. A 85, 042318 (2012).

T. Fogarty et al, Phys. Rev. A 87, 050304(R) (2013).

B. G. Taketani et al, Phys. Rev. A 90, 012312 (2014)